Author(s): Ge, Zhuang; Eronen, Tommi; Sevestrean, Vasile Alin; Niţescu, Ovidiu; Stoica, Sabin; Ramalho, Marlom; Suhonen, Jouni; de Roubin, Antoine; Nesterenko, Dmitrii; Kankainen, Anu; Ascher, Pauline; Ayet, San Andres Samuel; Beliuskina, Olga; Delahaye, Pierre; Flayol, Mathieu; Gerbaux, Mathias; Grévy, Stéphane; Hukkanen, Marjut; Jaries, Arthur; Jokinen, Ari; Husson, Audric; Kahl, Daid;

Title: High-precision measurements of the atomic mass and electron-capture decay Q value of 95Tc

Year: 2024

Version: Published version

Phys. Lett. B 859 (2024) 139094

Contents lists available at ScienceDirect

Physics Letters B

journal homepage: www.elsevier.com/locate/physletb

Letter

High-precision measurements of the atomic mass and electron-capture decay Q value of ^{95}Tc

Zhuang Ge [a,*], Tommi Eronen [a], Vasile Alin Sevestrean [b,c,d,**], Ovidiu Nițescu [b,d], Sabin Stoica [b], Marlom Ramalho [a], Jouni Suhonen [a,b,*], Antoine de Roubin [e,f], Dmitrii Nesterenko [a], Anu Kankainen [a], Pauline Ascher [f], Samuel Ayet San Andres [g], Olga Beliuskina [a], Pierre Delahaye [h], Mathieu Flayol [f], Mathias Gerbaux [f], Stéphane Grévy [f], Marjut Hukkanen [a,i], Arthur Jaries [a], Ari Jokinen [a], Audric Husson [f], Daid Kahl [j,l], Joel Kostensalo [k], Jenni Kotila [b,l,m], Iain Moore [a], Stylianos Nikas [a], Marek Stryjczyk [a], Ville Virtanen [a]

[a] Department of Physics, University of Jyväskylä, P.O. Box 35, FI-40014, Jyväskylä, Finland
[b] International Centre for Advanced Training and Research in Physics (CIFRA), POB MG-12, RO-077125, Bucharest-Măgurele, Romania
[c] Faculty of Physics, University of Bucharest, 405 Atomiştilor, POB MG-11, RO-077125, Bucharest-Măgurele, Romania
[d] "Horia Hulubei" National Institute of Physics and Nuclear Engineering, 30 Reactorului, POB MG-6, RO-077125, Bucharest-Măgurele, Romania
[e] KU Leuven, Instituut voor Kern- en Stralingsfysica, B-3001, Leuven, Belgium
[f] Université de Bordeaux, CNRS/IN2P3, UMR 5797, F-33170, Gradignan, France
[g] Instituto de Fisica Corpuscular, CSIC-UV, 46980, Gradignan, Spain
[h] GANIL, CEA/DSM-CNRS/IN2P3, Bd Henri Becquerel, 14000, Caen, France
[i] Université de Bordeaux, CNRS/IN2P3, LP2I Bordeaux, UMR 5797, F-33170, Gradignan, France
[j] Extreme Light Infrastructure - Nuclear Physics, Horia Hulubei National Institute for R&D in Physics and Nuclear Engineering (IFIN-HH), 077125, Bucharest-Magurele, Romania
[k] Natural Resources Institute Finland, Yliopistokatu 6B, FI-80100, Joensuu, Finland
[l] Finnish Institute for Educational Research, University of Jyväskylä, P.O. Box 35, FI-40014, Jyväskylä, Finland
[m] Center for Theoretical Physics, Sloane Physics Laboratory, Yale University, New Haven, CT 06520-8120, USA

ARTICLE INFO

Editor: H. Gao

Keywords:
Penning trap
Mass measurements
Ultra-low Q value
Electron capture

ABSTRACT

A direct measurement of the ground-state-to-ground-state electron-capture decay Q value of ^{95}Tc has been performed utilizing the double Penning trap mass spectrometer JYFLTRAP. The Q value was determined to be 1695.92(13) keV by taking advantage of the high resolving power of the phase-imaging ion-cyclotron-resonance technique to resolve the low-lying isomeric state of ^{95}Tc (excitation energy of 38.910(40) keV) from the ground state. The mass excess of ^{95}Tc was measured to be −86015.95(18) keV/c^2, exhibiting a precision of about 28 times higher and in agreement with the value from the newest Atomic Mass Evaluation (AME2020). Combined with the nuclear energy-level data for the decay-daughter ^{95}Mo, two potential ultra-low Q-value transitions are identified for future long-term neutrino-mass determination experiments. The atomic self-consistent many-electron Dirac–Hartree–Fock–Slater method and the nuclear shell model have been used to predict the partial half-lives and energy-release distributions for the two transitions. The dominant correction terms related to those processes are considered, including the exchange and overlap corrections, and the shake-up and shake-off effects. The normalized distribution of the released energy in the electron-capture decay of ^{95}Tc to excited states of ^{95}Mo is compared to that of ^{163}Ho currently being used for electron-neutrino-mass determination.

* Corresponding authors at: Department of Physics, University of Jyväskylä, P.O. Box 35, FI-40014, Jyväskylä, Finland.
** Corresponding author at: International Centre for Advanced Training and Research in Physics (CIFRA), POB MG-12, RO-077125, Bucharest-Măgurele, Romania.
E-mail addresses: zhuang.z.ge@jyu.fi (Z. Ge), sevestrean.alin@theory.nipne.ro (V.A. Sevestrean), jouni.t.suhonen@jyu.fi (J. Suhonen).
[1] Present address: Facility for Rare Isotope Beams, Michigan State University, 640 South Shaw Lane East Lansing, MI 48824, USA.

https://doi.org/10.1016/j.physletb.2024.139094
Received 7 June 2024; Received in revised form 18 August 2024; Accepted 22 October 2024
Available online 24 October 2024

Neutrino oscillations in atmospheric, solar, and reactor neutrinos have confirmed that at least two neutrino mass eigenstates have non-zero rest mass. However, these oscillations cannot assess the absolute mass scale, but only the squared differences of the mass eigenstates [1–3]. Neutrinos are the second most abundant particles in the universe, and play an important role on cosmological scales [4]. Accurate measurements of the total neutrino mass involve their imprint on the cosmic microwave background (CMB) as well as on structure formation in the early universe.

The most direct method to measure the absolute mass scale of antineutrinos involves studying the electron energy spectrum of β^- decay. Though the neutrinoless double β^--decay experiments can be used to infer the effective Majorana-neutrino mass from the measured lifetime, the exact relation depends on the mediator model and relies on the calculation of the involved transition matrix elements [5–8]. The ongoing leading experiment for the absolute neutrino mass scale determination is the Karlsruhe Tritium Neutrino (KATRIN) β^--decay experiment [9–11] which is designed to measure the electron-antineutrino mass, $m_{\overline{\nu}_e}$, with a sensitivity of 0.2 eV/c^2 at 90% C.L. Most recently, KATRIN has set a limit of $m_{\overline{\nu}_e} < 0.45$ eV/c^2 (90% C.L.) [12]. Another experiment, Project 8, takes advantage of the cyclotron radiation emission spectroscopy (CRES) technique via measurements of the tritium end-point spectrum. The new technique CRES will allow for an eventual sensitivity to $m_{\overline{\nu}_e}$ down to 0.04 eV/c^2. The first frequency-based neutrino mass limit of electron-weighted neutrino mass < 155 eV/c^2 is extracted from the background-free measurement of the continuous tritium β spectrum in a Bayesian (frequentist) analysis [13]. An alternative method in the ECHo [14–17] and HOLMES [18,19] experiments, uses electron capture (EC) on ^{163}Ho, and has reached a current limit of 150 eV/c^2 for the electron-neutrino mass [16].

A Q value as small as possible is desired in these single decay experiments for electron (anti)neutrino mass determination. The effective fraction of decays in a given energy interval ΔE at the endpoint area will be larger with a lower Q value [20,21]. Currently, only ground-state-to-ground-state (gs-to-gs) decay cases ^{3}H (β decay) and ^{163}Ho (electron capture), are being used for direct neutrino-mass-determination experiments. Ongoing intensive searches for isotopes undergoing β/EC decays from the ground state to an excited state with a low Q value are actively conducted at JYFLTRAP, LEBIT, CPT, ISOTRAP and SHIPTRAP Penning traps [22–37]. Penning trap mass spectrometry (PTMS) is the leading technique for accurate and precise mass and Q value determination, and it is hitherto the only direct method to measure the decay Q value to a sub-keV precision or better to verify whether a potential candidate is an ultra-low (< 1 keV) Q-value transition or not. If an ultra-low Q-value EC/β transition is identified with a sufficiently high decay rate, the idea that involves operating mechanical quantum sensors to reach the required sensitivity as proposed in [38] could be used for the neutrino mass measurement.

In this article, we report on the first direct measurement of the gs-to-gs EC Q value of ^{95}Tc with JYFLTRAP PTMS. The precise Q value obtained in this study, in conjunction with nuclear energy level data for excited states of ^{95}Mo, is utilized to ascertain their ground-state-to-excited-state (gs-to-es) Q values. In the case of ^{95}Tc, there are two potential low Q-value gs-to-es EC transitions, that could be used for neutrino-mass detection. To explore this potential, we have utilized two computational approaches, the atomic self-consistent many-electron Dirac–Hartree–Fock–Slater method and the nuclear shell model, to predict the partial half-lives and energy-release distributions for the EC-decay transitions in question.

1. Experimental method

The experiment was performed at the Ion Guide Isotope Separator On-Line facility (IGISOL) using JYFLTRAP double Penning trap mass spectrometer [39] at the University of Jyväskylä, Finland [40,41].

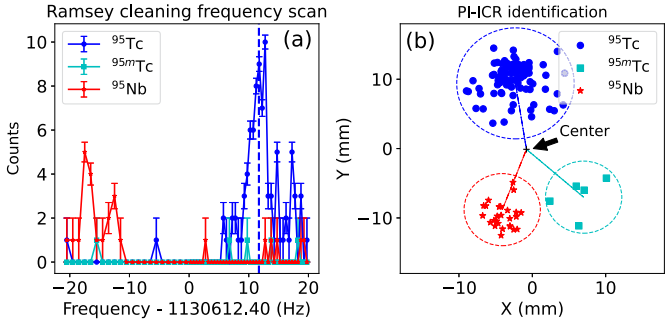

Fig. 1. (a) Ramsey-type dipole excitation frequency scan with a 5 ms (On) - 17 ms (Off) - 5 ms (On) excitation pattern in the second trap filtered by the positional gates shown in (b) using the PI-ICR identification (755 ms phase accumulation time) plot. The used angular gates are highlighted. The vertical dashed blue line shows the chosen optimal frequency to transmit ^{95}Tc ions while suppressing the others.

To generate ^{95}Tc ions, a natural Mo target foil was irradiated with a few μA proton beam at 45 MeV from the K-130 cyclotron at the Accelerator Laboratory of the University of Jyväskylä. A helium-filled small volume gas cell was used to stop the recoils produced from the proton-induced fusion-evaporation reaction, and the ions were extracted using gas flow and guided through a sextupole ion guide [42] with a combination of DC and RF fields. Subsequently, the ions were accelerated with a 30 kV electric potential, followed by mass separation using a 55° dipole magnet with a typical mass resolving power of $M/\Delta M \approx 500$. After isobaric separation for ions of $A/q = 95$, including the reaction products ^{95}Nb$^+$, ^{95m}Tc$^+$, ^{95}Tc$^+$ and ^{95}Mo$^+$, they were directed to a radiofrequency-quadrupole cooler-buncher (RFQ-CB) [43], where they underwent accumulation, cooling, and bunching.

Decay-daughter ions of ^{95}Mo$^+$ were prepared using the upstairs offline glow-discharge ion source. A 90° electrostatic bender selected ions either from the online target station or the offline ion source for downstream transmission.

JYFLTRAP comprises two cylindrical Penning traps in a 7-T superconducting solenoid. The first trap, functioning as a purification trap, is filled with helium buffer gas and is used for isobaric purification through the sideband buffer gas cooling technique [44]. This method achieves purification with a mass resolving power of $\approx 10^5$. In the purification trap, all cooled and centered ions (^{95}Nb$^+$, ^{95m}Tc$^+$, ^{95}Tc$^+$, and ^{95}Mo$^+$) are initially excited to a large magnetron motion orbit. This is accomplished by applying a dipole excitation at the magnetron motion frequency ν_- for approximately 11 ms. Subsequently, a quadrupole excitation is executed for approximately 100 ms to center the ions of interest through collisions with the buffer gas. The buffer gas cooling technique eliminated ^{95}Mo$^+$ but did not have enough mass resolving power to remove the other aforementioned ions. To prepare mono-isotopic samples of ^{95}Tc$^+$, the coupling of the dipolar excitation with Ramsey's method of time-separated oscillatory fields [45] and the phase-imaging ion-cyclotron-resonance (PI-ICR) technique [46,47] was utilized, as described in details in [35]. A plot of the Ramsey-type dipole excitation frequency scan with a 5 ms (On) - 17 ms (Off) - 5 ms (On) excitation pattern in the second (precision) trap, filtered by the positional gates using the PI-ICR identification with a 755 ms phase accumulation time, is shown in Fig. 1.

For Q-value measurements, the PI-ICR method is used to measure the cyclotron frequency, $\nu_c = qB/(2\pi m)$, where B is the magnetic field strength, q is the charge and m the mass of the stored ion. The PI-ICR technique [47] provides around 40 times better resolving power than the conventional time-of-flight ion-cyclotron-resonance (TOF-ICR) method [47–49]. Two timing patterns are needed for the determination of ν_c. The patterns differ only in their quadrupolar conversion pulse, separated in time by the defined phase-accumulation time, t_{acc}. The phase images of these two are projected onto a position-sensitive MCP detec-

tor after the trap. Additionally a center point, measured without any excitations, is needed for angle determination.

The angle between two phase images of the projected radial motions with respect to the center spot is denoted as $\alpha_c = \alpha_+ - \alpha_-$, where α_+ and α_- represent the polar angles of the cyclotron and magnetron motion phases. The cyclotron frequency ν_c is derived from: $\nu_c = (\alpha_c + 2\pi n_c)/2\pi t_{acc}$, where n_c represents the full number of revolutions made by the measured ions during the phase accumulation time t_{acc}. Different accumulation times for $^{95}Tc^+$ were utilized to unambiguously assign n_c. An accumulation time of 574 ms was employed for the actual measurements to determine the final ν_c for both $^{95}Tc^+$ and $^{95}Mo^+$ ions; the choice also ensures that any leaked isobaric contaminant would not overlap with the ions of interest. The positions of the phase spots for magnetron and cyclotron motion were carefully selected to maintain an angle α_c within a few degrees. This choice aimed to minimize the shift in the ν_c ratio of the $^{95}Tc^+$-$^{95}Mo^+$ pair due to the conversion of the cyclotron motion to magnetron motion and the possible distortion of the ion-motion projection onto the detector to a level well below 10^{-10} [48]. The excitation of the ν_+ delay was systematically scanned over one magnetron period, while the extraction delay varied over one cyclotron period. This accounted for any residual magnetron and cyclotron motion that might have shifted the different spots. The total data accumulation time of interleaved measurements of ν_c for $^{95}Tc^+$-$^{95}Mo^+$ ions was ≈ 4.9 hours, respectively.

The gs-to-gs electron-capture Q value, Q_{EC}, can be derived from the mass difference of the decay pair:

$$Q_{EC} = (M_p - M_d)c^2 = (R-1)(M_d - qm_e)c^2 + (R \cdot B_d - B_p), \quad (1)$$

where M_p and M_d represent the masses of the parent and daughter atoms, respectively, and R ($= \nu_{c,d}/\nu_{c,p}$) denotes their cyclotron frequency ratio for singly charged ions ($q = 1$), with m_e being the mass of an electron. The electron binding energies of the parent and daughter atoms, denoted as B_p and B_d, are neglected due to their small values (on the order of a few eV [50]), and R is close to 1. Since both the parent and daughter ions have the same A/q and their relative mass difference $\Delta M/M < 10^{-4}$, the mass-dependent error becomes negligible compared to the statistical uncertainty achieved in the measurements. Also, the contribution of uncertainty to the Q value from the mass uncertainty of the reference (daughter), which is 0.12 keV/c^2 for ^{95}Mo [51], can be neglected.

2. Results and discussion

The determination of Q_{EC} depends on the measured cyclotron frequency ratio R via Eq. (1). Two data sets for $^{95}Tc^+$-$^{95}Mo^+$ were collected. A full scanning measurement of the magnetron phase, cyclotron phase and center spot in sequence (one cycle) was completed in less than 5 minutes for each ion species. In the analysis, the position of each spot was fit with the maximum likelihood method. A few cycles were summed to have reasonable statistics for fitting. The phase angles were calculated accordingly to deduce the cyclotron frequencies of each ion species. The cyclotron frequency ν_c of the daughter $^{95}Mo^+$ as a reference was linearly interpolated to the time of the measurement of the parent $^{95}Tc^+$ (ion of interest) to deduce the cyclotron frequency ratio R. Only the bunches with less than five detected ions were considered in the data analysis in order to reduce a possible cyclotron frequency shift due to ion-ion interactions [56,57]. The count-rate related frequency shifts were not observed in the analysis. The temporal fluctuation of the magnetic field $\delta_B(\nu_c)/\nu_c = \Delta t \times 2.01(25) \times 10^{-12}$/min [46], where Δt is the time interval between two consecutive reference measurements, is considered in the final results. Contribution of temporal fluctuations of the magnetic field to the final frequency ratio uncertainty was less than 10^{-10} since the parent-daughter measurements were interleaved with $\Delta t < 10$ minutes. The frequency shifts in the PI-ICR measurement due to ion image distortions were well below the statistical uncertainty and thus ignored in the calculation of the final uncertainty. Furthermore,

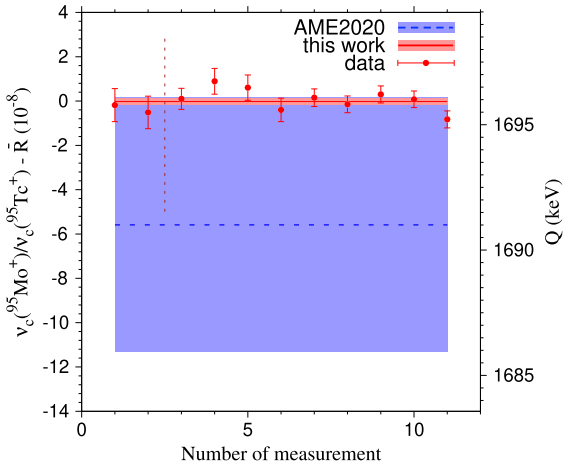

Fig. 2. The measured experimental results from this work compared to the literature values [59,51]. The deviations of the individually measured cyclotron frequency ratios R ($\nu_c(^{95}Mo^+)/\nu_c(^{95}Tc^+)$) from the measured value $\overline{R}$ (left axis) and Q value (right axis) in this work are compared to values adopted from AME2020. The red points with uncertainties represent individual measurements using the PI-ICR method. Vertical brown dashed lines separate measurements conducted at different time slots. The weighted average value $\overline{R}$ is depicted by the solid red line, and its 1σ uncertainty band is shaded in red. The dashed blue line illustrates the difference between our new value and the one referenced in AME2020, with its 1σ uncertainty area shaded in blue.

decay pair ions $^{95}Tc^+$-$^{95}Mo^+$, being mass doublets, cancel many of the systematic uncertainties in the cyclotron frequency ratio.

The weighted mean ratio $\overline{R}$ of all single ratios was calculated along with the inner and outer errors to deduce the Birge ratio [58]. The maximum of the inner and outer errors was taken as the weight to calculate $\overline{R}$. In Fig. 2, results of the analysis including all data with comparison to literature values are demonstrated. The final parent-to-daughter frequency ratio $\overline{R}$ with their uncertainty is determined to be 1.000 019 183 9(15). The corresponding gs-to-gs Q value is 1695.92(13) keV.

The gs-to-gs Q_{EC} value of 1695.92(13) keV from this work is ≈ 37 times more precise than that evaluated in AME2020 [59,51]. The measured Q_{EC} value has a deviation of 4.9(50) keV from the AME2020 value and is ≈1σ larger. The Q_{EC} value in AME2020 is derived primarily from two β^+-decay experiments $^{95}Tc(\beta^+)^{95}Mo$ [60,61]. Combined with the atomic mass of ^{95}Mo (mass excess: −87711.87(12) keV/c^2) from AME2020 [51,59], we deduce the mass excess of its parent nucleus ^{95}Tc ($9/2^+$) to be −86015.95(18) keV/c^2. The mass of ^{95}Tc in AME2020 is primarily evaluated from β^+-decay experiments $^{95}Tc(\beta^+)^{95}Mo$ and $^{95}Ru(\beta^+)^{95}Tc$ with influence of 97.4% and 2.6%, respectively [60,62,63].

The high-precision electron-capture energy from this work, together with the nuclear energy level data from Ref. [52–54] of the excited states of ^{95}Mo as tabulated in Table 1, was used to determine the gs-to-es Q (Q^*_{EC}) values of three candidate states as shown in Table 1. The newly determined Q^*_{EC} values confirm that the decay transitions of the ground state of ^{95}Tc to the three excited states of interest are energetically allowed.

In case of EC, the closer the Q value of the decay to one of the ionization energies of the captured electrons, the larger the resonance enhancement of the rate near the end-point, where the effects of a non-vanishing neutrino mass are relevant. The event-rate dependence on the Q value near the end-point for EC is steeper than that for β^- decay. As tabulated in Table 1, Δ_x gives the distance of the Q^*_{EC} value to the computed atomic relaxation energy ε_x following the capture of electrons in the allowed daughter atomic shells (x = K, L1, L2, and other electrons from s-levels and $p_{1/2}$-levels from the third and higher shells). For the state with the excitation energy of 1675.40(60) keV, the captures of electrons occupying the K and higher shells for the transition ^{95}Tc

Table 1
Potential candidate transitions of initial state (ground state) of parent nuclei ^{95}Tc ($9/2^+$) to the final states (excited states) of daughter ^{95}Mo with ultra-low Q values. The first column lists the excited final state of ^{95}Mo for the low Q value transition. The decay type is provided in the second column. The third and fourth columns present the derived decay $Q_{\rm EC}$ values in keV, sourced from literature (Lit.) [51] and this work (T. W.), respectively. The fifth column displays the experimental excitation energy E^* with its experimental error [52–54] in keV. The sixth column shows the confidence (σ) of the $Q^*_{\rm EC}$ being positive/negative. Columns seven to nine, denoted as Δx, represent the distance of $Q_{\rm EC}$ values to the computed atomic relaxation energy following the electron capture ε_x in the daughter atoms [55]. FNU means forbidden non-unique. Spin-parity assignments and energy values enclosed in braces {} signify uncertain assignments or uncertainties in excitation energy, resulting in uncertainties in the decay type or decay energy. All the energies are in unit of keV.

Final state	Decay type	$Q^*_{\rm EC}$ (Lit.)	$Q^*_{\rm EC}$ (T. W.)	E*	$Q/\delta Q$ (T. W.)	$\Delta_{\rm K}$ (T. W.)	$\Delta_{\rm L1}$ (T. W.)	$\Delta_{\rm L2}$ (T. W.)
^{95}Mo ($9/2^+$)	allowed	15.6(50)	20.52(61)	1675.40(60)	33	0.47(61)	17.64(61)	17.89(61)
^{95}Mo ({$7/2^+$, $9/2^+$})	{allowed}	8.0(51)	12.9(10)	1683.0(10)	13		10.0(10)	10.3(10)
^{95}Mo ($1/2^+$)	4th FNU	-1.0({51})	3.92({13})	1692({})	{29}		1.04({13})	1.29({13})

($9/2^+$) → ^{95}Mo* are energetically allowed, while for states with the excitation energy of 1683.0(10) keV and 1692 keV, only electrons from s-levels and $p_{1/2}$-levels from the second (L) and higher shells can possibly be captured due to angular momentum conservation and the finite overlap of their wave function with the nucleus. The transition ^{95}Tc ($9/2^-$) → ^{95}Mo* (1692 keV), giving the values of 1.04({13}) keV and 1.29({13}) keV for the distance of $Q^*_{\rm EC}$ to the computed atomic relaxation energy following the electron capture $\varepsilon_{L1} = 2.878$ keV and $\varepsilon_{L2} = 2.632$ keV, is of the decay type of 4$^{\rm th}$ FNU (forbidden non-unique). It has a long half-life which will result in an extremely low fraction of events landing near the endpoint. This transition is not of interest for future neutrino mass determination due to the low branching ratio. To confirm whether the emitted neutrino energy 1.04({13}) keV is ultra-low, further high-precision measurements of the excitation energy of the state are required. The parity of the 1683.0(10) keV state needs to be determined to verify the decay type of the transition to this state. The gs-to-gs Q value of ^{95}Tc is now well refined to sub keV uncertainty, combined with the energy level of 1675.40(60)-keV state, a possible ultra-low distance (0.47(61) keV) of $Q^*_{\rm EC}$ to the computed atomic relaxation energy following the electron capture $\varepsilon_k = 20.054$ keV [55] is observed to suggest it a suitable transition for potential neutrino mass measurements. Achieving precision below 100 eV for the 1675.40-keV state is highly desirable to unambiguously confirm whether the transition represents an energetically allowed decay.

3. Theoretical predictions

In the following we employed two calculation methods in order to predict the transition half-life and the distribution of energy released in the decay, namely atomic many-electron Dirac–Hartree–Fock–Slater (DHFS) self-consistent method and the Nuclear Shell Model (NSM) many-nucleon framework using the code NuShellX@MSU [64]. The DHFS framework has been proven adequate for this type of calculations in our previous work [65].

Using the DHFS method we obtained the wave-functions and the energy levels of the atomic electrons. The calculations were performed for both the initial atom and the final atom. The initial atom was in its ground state. For the final atom, we considered all possible states with the electron configuration of the initial atom having a hole in each shell from which the electron could be captured. For the atomic-structure calculations we made use of the RADIAL subroutine package [66], which also contains the DHFS.F code.

We denote the electron shell as $x = (n, \kappa)$, where n is the principal quantum number and κ is the relativistic quantum number. The atomic relaxation energy following the capture of an electron from the x shell is denoted as ε_x. It is calculated according to the refined energy conservation in [65], as $\varepsilon_x = |T_{\rm g.s.}| - |T_x|$, where $T_{\rm g.s.}$ and T_x are the total binding energy of the final atom in the ground state and in the excited state with a hole in the x shell.

For allowed transitions the energy distribution of an EC event is calculated as a sum over all atomic shells with $\kappa = \pm 1$ as

$$\rho(E) = \frac{G_\beta^2}{(2\pi)^2} C \sum_x n_x \beta_x^2 B_x S_x p_\nu E_\nu \frac{\Gamma_x/(2\pi)}{\left(E - \varepsilon_x\right)^2 + \Gamma_x^2/4}, \tag{2}$$

where B_x and S_x are the exchange and overlap corrections, and the shake-up and shake-off corrections, respectively, presented in detail in [65]. Here we go beyond the formalism used in [28] by adding the shake-up and shake-off corrections into the energy distribution $\rho(E)$. Here E is related to the energy of the neutrino E_ν and the Q value as $E = Q^*_{\rm EC} - E_\nu$. The momentum of the neutrino is denoted as $p_\nu = \sqrt{E_\nu^2 - m_\nu^2}$. The Coulomb amplitude is represented as β_x, while n_x is the relative occupancy of the shell. The intrinsic line-widths of Breit–Wigner resonances centered at ε_x are denoted as Γ_x and are taken from [67]. The Fermi constant $G_{\rm F}$ and the Cabibbo angle $\theta_{\rm C}$ are combined in $G_\beta = G_{\rm F} \cos\theta_{\rm C}$. For allowed transitions, the nuclear structure information is contained in the shape factor C in terms of the nuclear form factor ${}^A F_{101}^{(0)}$ [68]:

$$C = \left[{}^A F_{101}^{(0)}\right]^2 = \left[-\frac{g_{\rm A}}{\sqrt{2J_i + 1}} M_{\rm GT}\right]^2, \tag{3}$$

where $M_{\rm GT}$ is the Gamow–Teller nuclear matrix element [69]. The angular momentum of the initial nucleus is denoted as J_i, while the strength of the weak axial coupling is represented as $g_{\rm A}$.

For the $M_{\rm GT}$ calculation we used the NSM interactions *jj45pna* [70], a two-nucleon potential with a perturbative G-matrix approach with the single-particle energies adjusted in the Coulomb part to reproduce the recent results in [71] and *jj45pnb* [72], both sharing the same jj45pn model space. Additionally, we employed the interaction *glekpn* [73]. We computed the level scheme of the parent and daughter nuclei along with a few electromagnetic moments to evaluate the validity of three shell-model interactions. Our findings indicated that the *jj45pna* and *jj45pnb* interactions showed a stronger agreement with the available experimental data compared to the *glekpn*. Then, for the value of the weak axial coupling $g_{\rm A}$ we used the conservative range of 0.7 to 1 [74–76] and presented the partial half-life corresponding to the mean decay rate in Table 2. The mean rate corresponds to a $g_{\rm A}$ value equal to 0.857. The half-life for the values in the selected interval of $g_{\rm A}$ are between −33.3% and +36.1% of each mean value.

The total decay constantλ is obtained by integrating the energy distribution over the entire energy range $(0, Q^*_{\rm EC} - m_\nu)$. Using the narrow-width approximation, the decay rate can be written as:

$$\lambda = \frac{G_\beta^2}{(2\pi)^2} C \sum_x n_x \beta_x^2 B_x S_x p_{\nu x} \left(Q^*_{\rm EC} - \varepsilon_x\right), \tag{4}$$

where $p_{\nu x} = \sqrt{\left(Q^*_{\rm EC} - \varepsilon_x\right)^2 - m_\nu^2}$.

Table 2
Computed mean half-lives using $g_A = 0.857$ (see the main text) for the EC decay of ^{95}Tc to the two excited states in ^{95}Mo (with experimental energies $E^* = 1675.4$ keV and 1683 keV), using three shell-model interactions for the Gamow-Teller matrix element, with their experimental Q values shown in column 1. The second column indicates the used interactions and the third column the Gamow–Teller nuclear matrix element [69]. The computed total half-life and partial half-lives are demonstrated in columns 4-12. The atomic subshells are denoted using the X-ray notation.

Q^*_{EC} (keV)	interaction	M_{GT}	Total half-life (10^3yr)	K (10^7yr)	L1 (10^4yr)	L2 (10^5yr)	M1 (10^4yr)	M2 (10^6yr)	N1 (10^5yr)	N2 (10^7yr)	O1 (10^6yr)
20.52	jj45pna	−0.00696	877	20.0	117	708	640	267	223	146	491
	jj45pnb	-0.016533	155	3.55	20.8	125	81.6	47.4	39.4	25.8	87.1
	glekpn	0.0070667	850	19.4	114	587	446	259	216	141	477
12.9	jj45pna	−0.02412	173	-	24.1	143	79.7	46.0	37.5	24.5	82.6
	jj45pnb	-0.0198667	255	-	35.6	210	117	67.9	55.3	36.1	122
	glekpn	0.2296	1.9	-	0.266	1.57	0.880	0.508	0.414	0.271	0.911

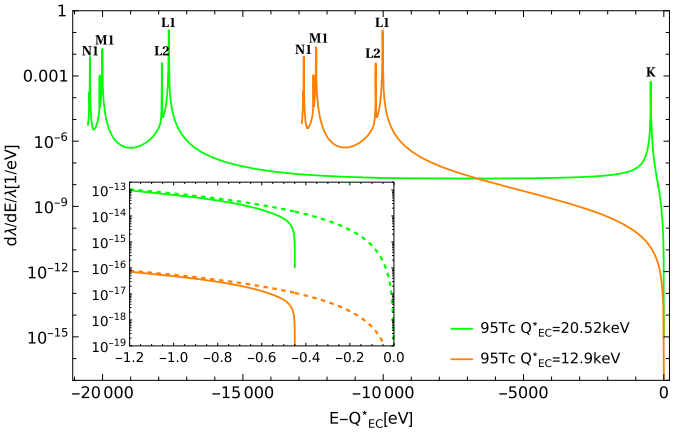

Fig. 3. Normalized distributions of released energy in the EC decay of ^{95}Tc in the transitions to the excited states of ^{95}Mo, as functions of $E - Q^*_{EC}$. The experimental excitation energies are $E^* = 1675.40$ keV and $E^* = 1683.0$ keV, while the corresponding Q values are $Q^*_{EC} = 20.52$ keV (green) and $Q^*_{EC} = 12.9$ keV (orange). The K, L1, L2, M1 and N1 notations indicate sub-shells from which the electron was captured. The M2, N2 and O1 sub-shells are harder to distinguish and are not labeled. The inset indicates an enlarged endpoint region showing the effect of neutrino masses of 0.45 eV and 0 eV. The dotted lines depict the spectra for a massless neutrino, while the solid lines correspond to a neutrino mass of 0.45 eV.

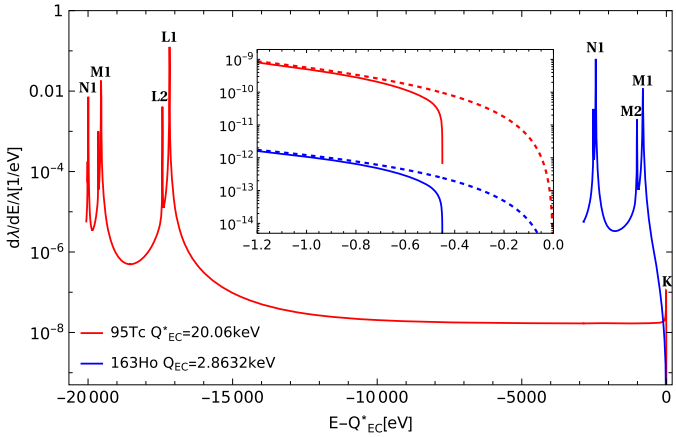

Fig. 4. Normalized distribution of released energy in the EC decay of ^{95}Tc in the transition to the excited state $E^* = 1675.40$ keV of ^{95}Mo, with $Q^*_{EC} = 20.06$ keV, as function of $E - Q^*_{EC}$ in comparison to that of ^{163}Ho with gs-to-gs $Q_{EC} = 2.8632$ keV [78]. The red line corresponds to the on-resonance EC decay using the experimental Q^*_{EC} of 20.06 keV within 1σ range of the central value 20.52 keV, while the blue line corresponds to the Q^*_{EC} of 2.8632 keV. For the sub-shell notation and the inset the reader is referred to the caption of Fig. 3.

While an electron is captured by the nucleus, the other electrons (the spectator electrons) can undergo some processes which affect the decay rate. Multiple corrections, including exchange, overlap, shake-up, and shake-off effects, were considered as explained in detail in a forthcoming theory paper [77].

The energy levels of the daughter nucleus were computed to identify the theoretical states corresponding to the experimental states of interest (1675.4 keV, 1683 keV). We compared the theoretical energies with the experimental ones and concluded that the following are the theoretical states closest to the experimental ones: for the experimental state with $J_f = 9/2$ and $E^* = 1675.4$ keV the best matches were $E^*_{th} = 1748$ keV for *jj45pna*, $E^*_{th} = 1897$ keV for *jj45pnb*, and $E^*_{th} = 1703$ keV for *glekpn*. All the mentioned theoretical states have $J_f = 9/2$. For the experimental state having the energy $E^* = 1683$ keV and with the angular momentum and parity uncertain $\{7/2^+, 9/2^+\}$, the closest correspondence is for *jj45pna* the energy $E^*_{th} = 1584$ keV, for *jj45pnb* the energy $E^*_{th} = 1642$ keV, and for *glekpn* the energy $E^*_{th} = 1707$ keV. The mentioned three theoretical states have the angular momentum and parity $7/2^+$.

In Table 2, we present the predicted half-lives for the decay of ^{95}Tc to the two excited states of ^{95}Mo for all relevant atomic shells. In Fig. 3 the normalized distribution of the released energy in the EC decay of ^{95}Tc to excited states of ^{95}Mo is demonstrated. The transition spectrum of ^{95}Tc $(9/2^+) \rightarrow {}^{95}$Mo* (1675.4 keV) is indicated in green, with Q^*_{EC} of 20.52 keV, situated 0.47 keV relative to the computed atomic relaxation energy following the electron capture in the allowed K shell. In contrast, the transition ^{95}Tc $(9/2^+) \rightarrow {}^{95}$Mo* (1683.0 keV), shown in orange, with a Q^*_{EC} value of 12.9 keV, is relatively farther from the computed atomic relaxation energy following the electron capture of the allowed L1 shell (giving a value of 10 keV for the distance). As illustrated in the inset of Fig. 3, a more pronounced resonance enhancement in the last 0.45 eV region near the endpoint for the former transition is observed, suggesting a preference for choosing this transition as a candidate for determining a non-vanishing neutrino mass. This phenomenon guides us to search for cases that have the smallest distance of Q^*_{EC} to the highest ionization energy of the captured electron of all allowed shells for neutrino-mass determination experiments.

The decay rate close to the endpoint is highly sensitive to small variations of the Q value as demonstrated by the K level, manifesting as a resonance itself, and thus can radically increase the number of recorded events near the endpoint. The current accuracy of measurement of the Q^*_{EC} value does not allow to make an unambiguous conclusion about the position of the $1s$ level, relative to the endpoint. Assuming $Q_{EC^*} = 20.06$ keV, which is consistent with the 1σ range of experimental error and is shifted by -0.46 keV relative to the central value, the resonance at the endpoint provides the highest EC event rate in the neutrino-mass sensitive region. Fig. 4 shows the normalized EC energy spectrum as a function of the energy, $E - Q^*_{EC}$, deposited in a calorimeter through the de-excitation of atomic shells for $Q^*_{EC} = 20.06$ keV, in comparison to the EC energy spectra in ^{163}Ho atom. The $s1$ level, K, has a significant EC counting-rate enhancement for the transition ^{95}Tc $(9/2^+) \rightarrow {}^{95}$Mo* (1675.40 keV) in the neutrino-mass sensitive region, as shown on an en-

larged scale in the inset of Fig. 4. Assuming a Q value of $Q^*_{\mathrm{EC}} = 20.06$ keV, technetium is about three orders of magnitude more effective than holmium. Based on these findings, it can be conjectured that we have found a potentially strong transition for direct electron-neutrino mass determination. However, the short half-life of about 1 day for the ^{95}Tc can prove to be a challenge experimentally.

4. Conclusion and outlook

A direct high-precision gs-to-gs EC-decay Q-value measurement of ^{95}Tc $(9/2^+) \rightarrow {}^{95}$Mo $(5/2^+)$ was performed using the PI-ICR technique at JYFLTRAP Penning trap mass spectrometer. A Q value of 1695.92(13) keV was obtained and the precision was improved by a factor of around 37 compared to literature. The measurement also improved the mass excess of ^{95}Tc by a factor of 28 compared to previous experiments. Three candidate transitions of ^{95}Tc $(9/2^+) \rightarrow {}^{95}$Mo* were validated to be energetically allowed. The refined sub-keV precision of the gs-to-gs Q value of ^{95}Tc allows us to find a possible ultra-low energy difference (0.47(61) keV) between Q^*_{EC} and the atomic relaxation energy $\epsilon_k = 20.054$ keV in the K capture for the allowed gs-to-es transition to the 1675.40-keV state. The spin of the 1683.0-keV state needs to be determined along with its energy with higher precision in order to see if the related transition is allowed and of low Q value.

The atomic self-consistent many-electron Dirac–Hartree–Fock–Slater method and three nuclear shell-model interactions were utilized to predict the partial decay half-lives and energy distributions of gs-to-es EC transitions in ^{95}Tc with low Q values. We computed the energy levels of the parent and daughter nuclei and a few electromagnetic moments to assess the validity of the three shell-model interactions (*jj45pna*, *jj45pnb*, *glekpn*). Multiple corrections, such as exchange, overlap, shake-up, and shake-off effects, were accounted for in these predictions. From the calculations, the possible ultra-low distance to the atomic line K, level 1s, for ^{95}Tc $(9/2^+) \rightarrow {}^{95}$Mo* (1675.40 keV) results in a significant increase in the number of EC events in the energy region sensitive to the electron neutrino mass. These findings confirm a potentially powerful transition for direct electron-neutrino mass determination.

Declaration of competing interest

The authors declare that they have no known competing financial interests or personal relationships that could have appeared to influence the work reported in this paper.

Acknowledgements

We acknowledge the staff of the Accelerator Laboratory of University of Jyväskylä (JYFL-ACCLAB) for providing stable online beam. We thank the support by the Research Council of Finland under the Finnish Centre of Excellence Programme 2012–2017 (Nuclear and Accelerator Based Physics Research at JYFL) and projects No. 306980, 312544, 275389, 284516, 295207, 314733, 315179, 327629, 320062, 354589, 345869 and 354968. The support by the EU Horizon 2020 research and innovation program under grant No. 771036 (ERC CoG MAIDEN) is acknowledged. This project has received funding from the European Union's Horizon 2020 research and innovation programme under grant agreement No. 861198–LISA–H2020-MSCA-ITN-2019. V.A.S., O.N., S.S., J.S., and J.K. acknowledge support from project PNRR-I8/C9-CF264, Contract No. 760100/23.05.2023 of the Romanian Ministry of Research, Innovation and Digitization. The work leading to this publication was supported by the Deutsche Forschungsgemeinschaft (DFG, German Research Foundation) - AY 155/2-1. The paper was supported by the DAAD Grant No. 57610603.

Data availability

Data will be made available on request.

References

[1] Y. Fukuda, T. Hayakawa, E. Ichihara, K. Inoue, K. Ishihara, H. Ishino, Y. Itow, T. Kajita, J. Kameda, S. Kasuga, K. Kobayashi, Y. Kobayashi, Y. Koshio, M. Miura, M. Nakahata, S. Nakayama, A. Okada, K. Okumura, N. Sakurai, M. Shiozawa, Y. Suzuki, Y. Takeuchi, Y. Totsuka, S. Yamada, M. Earl, A. Habig, E. Kearns, M.D. Messier, K. Scholberg, J.L. Stone, L.R. Sulak, C.W. Walter, M. Goldhaber, T. Barszczxak, D. Casper, W. Gajewski, P.G. Halverson, J. Hsu, W.R. Kropp, L.R. Price, F. Reines, M. Smy, H.W. Sobel, M.R. Vagins, K.S. Ganezer, W.E. Keig, R.W. Ellsworth, S. Tasaka, J.W. Flanagan, A. Kibayashi, J.G. Learned, S. Matsuno, V.J. Stenger, D. Takemori, T. Ishii, J. Kanzaki, T. Kobayashi, S. Mine, K. Nakamura, K. Nishikawa, Y. Oyama, A. Sakai, M. Sakuda, O. Sasaki, S. Echigo, M. Kohama, A.T. Suzuki, T.J. Haines, E. Blaufuss, B.K. Kim, R. Sanford, R. Svoboda, M.L. Chen, Z. Conner, J.A. Goodman, G.W. Sullivan, J. Hill, C.K. Jung, K. Martens, C. Mauger, C. Mc Grew, E. Sharkey, B. Viren, C. Yanagisawa, W. Doki, K. Miyano, H. Okazawa, C. Saji, M. Takahata, Y. Nagashima, M. Takita, T. Yamaguchi, M. Yoshida, S.B. Kim, M. Etoh, K. Fujita, A. Hasegawa, T. Hasegawa, S. Hatakeyama, T. Iwamoto, M. Koga, T. Maruyama, H. Ogawa, J. Shirai, A. Suzuki, F. Tsushima, M. Koshiba, M. Nemoto, K. Nishijima, T. Futagami, Y. Hayato, Y. Kanaya, K. Kaneyuki, Y. Watanabe, D. Kielczewska, R.A. Doyle, J.S. George, A.L. Stachyra, L.L. Wai, R.J. Wilkes, K.K. Young, Evidence for oscillation of atmospheric neutrinos, Phys. Rev. Lett. 81 (8) (1998) 1562–1567, https://doi.org/10.1103/PhysRevLett.81.1562, http://link.aps.org/doi/10.1103/PhysRevLett.81.1562, arXiv:hep-ex/9807003.

[2] SNO Collaboration, Direct evidence for neutrino flavor transformation from neutral-current interactions in the Sudbury neutrino observatory, Phys. Rev. Lett. 89 (1) (2002) 1–6, https://doi.org/10.1103/PhysRevLett.89.011301, arXiv:nucl-ex/0204008.

[3] M. Gerbino, M. Lattanzi, Status of neutrino properties and future prospects—cosmological and astrophysical constraints, Front. Phys. 5 (2018), https://doi.org/10.3389/fphy.2017.00070.

[4] E. Giusarma, M. Reyes, F. Villaescusa-Navarro, S. He, S. Ho, C. Hahn, Learning neutrino effects in cosmology with convolutional neural network, Astrophys. J. 950 (1) (2023) 70, https://doi.org/10.3847/1538-4357/accd61.

[5] J. Suhonen, O. Civitarese, Weak-interaction and nuclear-structure aspects of nuclear double beta decay, Phys. Rep. 300 (3–4) (1998) 123–214, https://doi.org/10.1016/S0370-1573(97)00087-2.

[6] F.T. Avignone, S.R. Elliott, J. Engel, Double beta decay, Majorana neutrinos, and neutrino mass, Rev. Mod. Phys. 80 (2) (2008) 481–516, https://doi.org/10.1103/RevModPhys.80.481, http://link.aps.org/doi/10.1103/RevModPhys.80.481, arXiv:0708.1033.

[7] H. Ejiri, J. Suhonen, K. Zuber, Neutrino–nuclear responses for astro-neutrinos, single beta decays and double beta decays, Phys. Rep. 797 (2019) 1–102, https://doi.org/10.1016/j.physrep.2018.12.001.

[8] M. Agostini, G. Benato, J.A. Detwiler, J. Menéndez, F. Vissani, Toward the discovery of matter creation with neutrinoless $\beta\beta$ decay, Rev. Mod. Phys. 95 (2023) 025002, https://doi.org/10.1103/RevModPhys.95.025002, https://link.aps.org/doi/10.1103/RevModPhys.95.025002.

[9] G. Drexlin, V. Hannen, S. Mertens, C. Weinheimer, Current direct neutrino mass experiments, Adv. High Energy Phys. 2013 (i) (2013) 1–39, https://doi.org/10.1155/2013/293986, http://www.hindawi.com/journals/ahep/2013/293986/, arXiv:1307.0101.

[10] M. Aker, K. Altenmüller, M. Arenz, M. Babutzka, J. Barrett, S. Bauer, M. Beck, A. Beglarian, J. Behrens, T. Bergmann, U. Besserer, K. Blaum, F. Block, S. Bobien, K. Bokeloh, J. Bonn, B. Bornschein, L. Bornschein, H. Bouquet, T. Brunst, T.S. Caldwell, L. La Cascio, S. Chilingaryan, W. Choi, T.J. Corona, K. Debowski, M. Deffert, M. Descher, P.J. Doe, O. Dragoun, G. Drexlin, J.A. Dunmore, S. Dyba, F. Edzards, L. Eisenblätter, K. Eitel, E. Ellinger, R. Engel, S. Enomoto, M. Erhard, D. Eversheim, M. Fedkevych, A. Felden, S. Fischer, B. Flatt, J.A. Formaggio, F.M. Fränkle, G.B. Franklin, H. Frankrone, F. Friedel, D. Fuchs, A. Fulst, D. Furse, K. Gauda, H. Gemmeke, W. Gil, F. Glück, S. Görhardt, S. Groh, S. Grohmann, R. Grössle, R. Gumbsheimer, M. Ha Minh, M. Hackenjos, V. Hannen, F. Harms, J. Hartmann, N. Haußmann, F. Heizmann, K. Helbing, S. Hickford, D. Hilk, B. Hillen, D. Hillesheimer, D. Hinz, T. Höhn, B. Holzapfel, S. Holzmann, T. Houdy, M.A. Howe, A. Huber, T.M. James, A. Jansen, A. Kaboth, C. Karl, O. Kazachenko, J. Kellerer, N. Kernert, L. Kippenbrock, M. Kleesiek, M. Klein, C. Köhler, L. Köllenberger, A. Kopmann, M. Korzeczek, A. Kosmider, A. Kovalík, B. Krasch, M. Kraus, H. Krause, L. Kuckert, B. Kuffner, N. Kunka, T. Lasserre, T.L. Le, O. Lebeda, M. Leber, B. Lehnert, J. Letnev, F. Leven, S. Lichter, V.M. Lobashev, A. Lokhov, M. MacHatschek, E. Malcherek, K. Müller, M. Mark, A. Marsteller, E.L. Martin, C. Melzer, A. Menshikov, S. Mertens, L.I. Minter, S. Mirz, B. Monreal, P.I. Morales Guzmán, K. Müller, U. Naumann, W. Ndeke, H. Neumann, S. Niemes, M. Noe, N.S. Oblath, H.W. Ortjohann, A. Osipowicz, B. Ostrick, E. Otten, D.S. Parno, D.G. Phillips, P. Plischke, A. Pollithy, A.W. Poon, J. Pouryamout, M. Prall, F. Priester, M. Röllig, C. Röttele, P.C. Ranitzsch, O. Rest, R. Rinderspacher, R.G. Robertson, C. Rodenbeck, P. Rohr, C. Roll, S. Rupp, M. Ryšavý, R. Sack, A. Saenz, P. Schäfer, L. Schimpf, K. Schlösser, M. Schlösser, L. Schlüter, H. Schön, K. Schönung, M. Schrank, B. Schulz, J. Schwarz, H. Seitz-Moskaliuk, W. Seller, V. Sibille, D. Siegmann, A. Skasyrskaya, M. Slezák, A. Špalek, F. Spanier, M. Steidl, N. Steinbrink, M. Sturm, M. Suesser, M. Sun, D. Tcherniakhovski, H.H. Telle, T. Thümmler, L.A. Thorne, N. Titov, I. Tkachev, N. Trost, K. Urban, D. Vénos, K. Valerius, B.A. Vandevender, R. Vianden, A.P. Vizcaya Hernández, B.L. Wall, S. Wüstling, M. We-

ber, C. Weinheimer, C. Weiss, S. Welte, J. Wendel, K.J. Wierman, J.F. Wilkerson, J. Wolf, W. Xu, Y.R. Yen, M. Zacher, S. Zadorozhny, M. Zbořil, G. Zeller, Improved upper limit on the neutrino mass from a direct kinematic method by KATRIN, Phys. Rev. Lett. 123 (22) (2019) 1–11, https://doi.org/10.1103/PhysRevLett.123.221802, arXiv:1909.06048.

[11] M. Aker, A. Beglarian, J. Behrens, A. Berlev, U. Besserer, B. Bieringer, F. Block, B. Bornschein, L. Bornschein, M. Böttcher, T. Brunst, T.S. Caldwell, R.M.D. Carney, L.L. Cascio, S. Chilingaryan, W. Choi, K. Debowski, M. Deffert, M. Descher, D.D. Barrero, P.J. Doe, O. Dragoun, G. Drexlin, K. Eitel, E. Ellinger, R. Engel, S. Enomoto, A. Felden, J.A. Formaggio, F.M. Fränkle, G.B. Franklin, F. Friedel, A. Fulst, K. Gauda, W. Gil, F. Glück, R. Grössle, R. Gumbsheimer, V. Gupta, T. Höhn, V. Hannen, N. Haußmann, K. Helbing, S. Hickford, R. Hiller, D. Hillesheimer, D. Hinz, T. Houdy, A. Huber, A. Jansen, C. Karl, F. Kellerer, J. Kellerer, M. Klein, C. Köhler, L. Köllenberger, A. Kopmann, M. Korzeczek, A. Kovalík, B. Krasch, H. Krause, N. Kunka, T. Lasserre, T.L. Le, O. Lebeda, B. Lehnert, A. Lokhov, M. Machatschek, E. Malcherek, M. Mark, A. Marsteller, E.L. Martin, C. Melzer, A. Menshikov, S. Mertens, J. Mostafa, K. Müller, S. Niemes, P. Oelpmann, D.S. Parno, A.W.P. Poon, J.M.L. Poyato, F. Priester, M. Röllig, C. Röttele, R.G.H. Robertson, W. Rodejohann, C. Rodenbeck, M. Ryšavý, R. Sack, A. Saenz, P. Schäfer, A. Schaller, L. Schimpf, K. Schlösser, M. Schlösser, L. Schlüter, S. Schneidewind, M. Schrank, B. Schulz, A. Schwemmer, M. Šefčík, V. Sibille, D. Siegmann, M. Slezák, M. Steidl, M. Sturm, M. Sun, D. Tcherniakhovski, H.H. Telle, L.A. Thorne, T. Thümmler, N. Titov, I. Tkachev, K. Urban, K. Valerius, D. Vénos, A.P.V. Hernández, C. Weinheimer, S. Welte, J. Wendel, J.F. Wilkerson, J. Wolf, S. Wüstling, W. Xu, Y.R. Yen, S. Zadoroghny, G. Zeller, Direct neutrino-mass measurement with sub-electronvolt sensitivity, Nat. Phys. 18 (2022) 160, https://doi.org/10.1038/s41567-021-01463-1.

[12] M. Aker, D. Batzler, A. Beglarian, J. Behrens, J. Beisenkötter, M. Biassoni, B. Bieringer, Y. Biondi, F. Block, S. Bobien, M. Böttcher, B. Bornschein, L. Bornschein, T.S. Caldwell, M. Carminati, A. Chatrabhuti, S. Chilingaryan, B.A. Daniel, K. Debowski, M. Descher, D.D. Barrero, P.J. Doe, O. Dragoun, G. Drexlin, F. Edzards, K. Eitel, E. Ellinger, R. Engel, S. Enomoto, A. Felden, C. Fengler, C. Fiorini, J.A. Formaggio, C. Forstner, F.M. Fränkle, K. Gauda, A.S. Gavin, W. Gil, F. Glück, S. Grohmann, R. Grössle, R. Gumbsheimer, N. Gutknecht, V. Hannen, L. Hasselmann, N. Haußmann, K. Helbing, H. Henke, S. Heyns, S. Hickford, R. Hiller, D. Hillesheimer, D. Hinz, T. Höhn, A. Huber, A. Jansen, C. Karl, J. Kellerer, K. Khosonthongkee, M. Kleifges, M. Klein, J. Kohpeiß, C. Köhler, L. Köllenberger, A. Kopmann, N. Kovač, A. Kovalík, H. Krause, L.L. Cascio, T. Lasserre, J. Lauer, T. Le, O. Lebeda, B. Lehnert, G. Li, A. Lokhov, M. Machatschek, M. Mark, A. Marsteller, E.L. Martin, C. Melzer, S. Mertens, S. Mohanty, J. Mostafa, K. Müller, A. Nava, H. Neumann, S. Niemes, A. Onillon, D.S. Parno, M. Pavan, U. Pinsook, A.W.P. Poon, J.M.L. Poyato, S. Pozzi, F. Priester, J. Ráliš, S. Ramachandran, R.G.H. Robertson, C. Rodenbeck, M. Röllig, C. Röttele, M. Ryšavý, R. Sack, A. Saenz, R. Salomon, P. Schäfer, M. Schlösser, K. Schlösser, L. Schlüter, S. Schneidewind, U. Schnurr, M. Schrank, J. Schürmann, A. Schütz, A. Schwemmer, A. Schwenck, M. Šefčík, D. Siegmann, F. Simon, F. Spanier, D. Spreng, W. Sreethawong, M. Steidl, J. Štorek, X. Stribl, M. Sturm, N. Suwonjandee, N.T. Jerome, H.H. Telle, L.A. Thorne, T. Thümmler, S. Tirolf, N. Titov, I. Tkachev, K. Urban, K. Valerius, D. Vénos, C. Weinheimer, S. Welte, J. Wendel, C. Wiesinger, J.F. Wilkerson, J. Wolf, S. Wüstling, J. Wydra, W. Xu, S. Zadorozhny, G. Zeller, Direct neutrino-mass measurement based on 259 days of katrin data, arXiv:2406.13516, 2024.

[13] A. Ashtari Esfahani, S. Böser, N. Buzinsky, M.C. Carmona-Benitez, C. Claessens, L. de Viveiros, P.J. Doe, M. Fertl, J.A. Formaggio, J.K. Gaison, L. Gladstone, M. Grando, M. Guigue, J. Hartse, K.M. Heeger, X. Huyan, J. Johnston, A.M. Jones, K. Kazkaz, B.H. LaRoque, M. Li, A. Lindman, E. Machado, A. Marsteller, C. Matthé, R. Mohiuddin, B. Monreal, R. Mueller, J.A. Nikkel, E. Novitski, N.S. Oblath, J.I. Peña, W. Pettus, R. Reimann, R.G.H. Robertson, D. Rosa De Jesús, G. Rybka, L. Saldaña, M. Schram, P.L. Slocum, J. Stachurska, Y.H. Sun, P.T. Surukuchi, J.R. Tedeschi, A.B. Telles, F. Thomas, M. Thomas, L.A. Thorne, T. Thümmler, L. Tvrznikova, W. Van De Pontseele, B.A. VanDevender, J. Weintroub, T.E. Weiss, T. Wendler, A. Young, E. Zayas, A. Ziegler, Project 8 Collaboration, Tritium beta spectrum measurement and neutrino mass limit from cyclotron radiation emission spectroscopy, Phys. Rev. Lett. 131 (2023) 102502, https://doi.org/10.1103/PhysRevLett.131.102502, https://link.aps.org/doi/10.1103/PhysRevLett.131.102502.

[14] L. Gastaldo, K. Blaum, A. Doerr, C.E. Düllmann, K. Eberhardt, S. Eliseev, C. Enss, A. Faessler, A. Fleischmann, S. Kempf, M. Krivoruchenko, S. Lahiri, M. Maiti, Y.N. Novikov, P.C. Ranitzsch, F. Simkovic, Z. Szusc, M. Wegner, The electron capture 163Ho experiment ECHo, J. Low Temp. Phys. 176 (5–6) (2014) 876–884, https://doi.org/10.1007/s10909-014-1187-4, arXiv:1306.2655.

[15] L. Gastaldo, K. Blaum, K. Chrysalidis, T. Day Goodacre, A. Domula, M. Door, H. Dorrer, C.E. Düllmann, K. Eberhardt, S. Eliseev, C. Enss, A. Faessler, P. Filianin, A. Fleischmann, D. Fonnesu, L. Gamer, R. Haas, C. Hassel, D. Hengstler, J. Jochum, K. Johnston, U. Kebschull, S. Kempf, T. Kieck, U. Köster, S. Lahiri, M. Maiti, F. Mantegazzini, B. Marsh, P. Neroutsos, Y.N. Novikov, P.C. Ranitzsch, S. Rothe, A. Rischka, A. Saenz, O. Sander, F. Schneider, S. Scholl, R.X. Schüssler, C. Schweiger, F. Simkovic, T. Stora, Z. Szücs, A. Türler, M. Veinhard, M. Weber, M. Wegner, K. Wendt, K. Zuber, The electron capture in 163Ho experiment – ECHo, Eur. Phys. J. Spec. Top. 226 (8) (2017) 1623–1694, https://doi.org/10.1140/epjst/e2017-70071-y, http://link.springer.com/10.1140/epjst/e2017-70071-y.

[16] C. Velte, F. Ahrens, A. Barth, K. Blaum, M. Braß, M. Door, H. Dorrer, C.E. Düllmann, S. Eliseev, C. Enss, P. Filianin, A. Fleischmann, L. Gastaldo, A. Goeggelmann, T.D. Goodacre, M.W. Haverkort, D. Hengstler, J. Jochum, K. Johnston, M. Keller, S. Kempf, T. Kieck, C.M. König, U. Köster, K. Kromer, F. Mantegazzini, B. Marsh, Y.N. Novikov, F. Piquemal, C. Riccio, D. Richter, A. Rischka, S. Rothe, R.X. Schüssler, C. Schweiger, T. Stora, M. Wegner, K. Wendt, M. Zampaolo, K. Zuber, High-resolution and low-background ^{163}Ho spectrum: interpretation of the resonance tails, Eur. Phys. J. C 79 (12) (2019), https://doi.org/10.1140/epjc/s10052-019-7513-x, http://link.springer.com/10.1140/epjc/s10052-019-7513-x.

[17] F. Mantegazzini, N. Kovac, C. Enss, A. Fleischmann, M. Griedel, L. Gastaldo, Development and characterisation of high-resolution microcalorimeter detectors for the echo-100k experiment, Nucl. Instrum. Methods Phys. Res., Sect. A, Accel. Spectrom. Detect. Assoc. Equip. 1055 (2023) 168564, https://doi.org/10.1016/j.nima.2023.168564, https://www.sciencedirect.com/science/article/pii/S0168900223005545.

[18] A. Nucciotti, B. Alpert, M. Balata, D. Becker, D. Bennett, A. Bevilacqua, M. Biasotti, V. Ceriale, G. Ceruti, D. Corsini, M. De Gerone, R. Dressler, M. Faverzani, E. Ferri, J. Fowler, G. Gallucci, J. Gard, F. Gatti, A. Giachero, J. Hays-Wehle, S. Heinitz, G. Hilton, U. Köster, M. Lusignoli, J. Mates, S. Nisi, A. Orlando, L. Parodi, G. Pessina, A. Puiu, S. Ragazzi, C. Reintsema, M. Ribeiro-Gomez, D. Schmidt, D. Schuman, F. Siccardi, D. Swetz, J. Ullom, L. Vale, Status of the Holmes experiment to directly measure the neutrino mass, J. Low Temp. Phys. 193 (5–6) (2018) 1137–1145, https://doi.org/10.1007/s10909-018-2025-x, arXiv:1807.09269.

[19] M. Borghesi, B. Alpert, M. Balata, D. Becker, D. Bennet, E. Celasco, N. Cerboni, M. De Gerone, R. Dressler, M. Faverzani, M. Fedkevych, E. Ferri, J. Fowler, G. Gallucci, J. Gard, F. Gatti, A. Giachero, G. Hilton, U. Koster, D. Labranca, M. Lusignoli, J. Mates, E. Maugeri, S. Nisi, A. Nucciotti, L. Origo, G. Pessina, S. Ragazzi, C. Reintsema, D. Schmidt, D. Schumann, D. Swetz, J. Ullom, L. Vale, An updated overview of the Holmes status, Nucl. Instrum. Methods Phys. Res., Sect. A, Accel. Spectrom. Detect. Assoc. Equip. 1051 (2023) 168205, https://doi.org/10.1016/j.nima.2023.168205, https://www.sciencedirect.com/science/article/pii/S016890022300195X.

[20] A.B. McDonald, G. Drexlin, V. Hannen, S. Mertens, C. Weinheimer, Current direct neutrino mass experiments, Adv. High Energy Phys. 2013 (2013) 293986, https://doi.org/10.1155/2013/293986.

[21] E. Ferri, D. Bagliani, M. Biasotti, G. Ceruti, D. Corsini, M. Faverzani, F. Gatti, A. Giachero, C. Gotti, C. Kilbourne, A. Kling, M. Maino, P. Manfrinetti, A. Nucciotti, G. Pessina, G. Pizzigoni, M. Ribeiro Gomes, M. Sisti, The status of the MARE experiment with 187Re and 163Ho isotopes, Phys. Proc. 61 (August 2015) 227–231, https://doi.org/10.1016/j.phpro.2014.12.037.

[22] J. Suhonen, Theoretical studies of rare weak processes in nuclei, Phys. Scr. 89 (5) (2014) 54032, https://doi.org/10.1088/0031-8949/89/5/054032, http://stacks.iop.org/1402-4896/89/i=5/a=054032.

[23] D.A. Nesterenko, S. Eliseev, K. Blaum, M. Block, S. Chenmarev, A. Dörr, C. Droese, P.E. Filianin, M. Goncharov, E. Minaya Ramirez, Y.N. Novikov, L. Schweikhard, V.V. Simon, Direct determination of the atomic mass difference of Re 187 and Os 187 for neutrino physics and cosmochronology, Phys. Rev. C, Nucl. Phys. 90 (4) (2014) 042501(R), https://link.aps.org/doi/10.1103/PhysRevC.90.042501, https://doi.org/10.1103/PhysRevC.90.042501.

[24] S. Eliseev, K. Blaum, M. Block, S. Chenmarev, H. Dorrer, C.E. Düllmann, C. Enss, P.E. Filianin, L. Gastaldo, M. Goncharov, U. Köster, F. Lautenschläger, Y.N. Novikov, A. Rischka, R.X. Schüssler, L. Schweikhard, A. Türler, Direct measurement of the mass difference of ^{163}Ho and ^{163}Dy solves the Q-value puzzle for the neutrino mass determination, Phys. Rev. Lett. 115 (6) (2015) 62501, https://doi.org/10.1103/PhysRevLett.115.062501, http://link.aps.org/doi/10.1103/PhysRevLett.115.062501, arXiv:1604.04210.

[25] J. Karthein, D. Atanasov, K. Blaum, S. Eliseev, P. Filianin, D. Lunney, V. Manea, M. Mougeot, D. Neidherr, Y. Novikov, L. Schweikhard, A. Welker, F. Wienholtz, K. Zuber, Direct decay-energy measurement as a route to the neutrino mass, Hyperfine Interact. 240 (1) (2019) 1–9, https://doi.org/10.1007/s10751-019-1601-z, http://link.springer.com/10.1007/s10751-019-1601-z, arXiv:1905.05510.

[26] A. De Roubin, J. Kostensalo, T. Eronen, L. Canete, R.P. De Groote, A. Jokinen, A. Kankainen, D.A. Nesterenko, I.D. Moore, S. Rinta-Antila, J. Suhonen, M. Vilén, High-precision Q -value measurement confirms the potential of Cs 135 for absolute antineutrino mass scale determination, Phys. Rev. Lett. 124 (22) (2020) 1–5, https://doi.org/10.1103/PhysRevLett.124.222503, arXiv:2002.08282.

[27] Z. Ge, T. Eronen, A. de Roubin, D.A. Nesterenko, M. Hukkanen, O. Beliuskina, R. de Groote, S. Geldhof, W. Gins, A. Kankainen, A. Koszorús, J. Kotila, J. Kostensalo, I.D. Moore, A. Raggio, S. Rinta-Antila, J. Suhonen, V. Virtanen, A.P. Weaver, A. Zadvornaya, A. Jokinen, Direct measurement of the mass difference of ^{72}As–^{72}Ge rules out ^{72}As as a promising β-decay candidate to determine the neutrino mass, Phys. Rev. C 103 (2021) 065502, https://doi.org/10.1103/PhysRevC.103.065502.

[28] Z. Ge, T. Eronen, K.S. Tyrin, J. Kotila, J. Kostensalo, D.A. Nesterenko, O. Beliuskina, R. de Groote, A. de Roubin, S. Geldhof, W. Gins, M. Hukkanen, A. Jokinen, A. Kankainen, A. Koszorús, M.I. Krivoruchenko, S. Kujanpää, I.D. Moore, A. Raggio, S. Rinta-Antila, J. Suhonen, V. Virtanen, A.P. Weaver, A. Zadvornaya, ^{159}Dy electron-capture: a new candidate for neutrino mass determination, Phys. Rev. Lett. 127 (2021) 272301, https://doi.org/10.1103/PhysRevLett.127.272301, https://link.aps.org/doi/10.1103/PhysRevLett.127.272301.

[29] Z. Ge, T. Eronen, A. de Roubin, K. Tyrin, L. Canete, S. Geldhof, A. Jokinen, A. Kankainen, J. Kostensalo, J. Kotila, M. Krivoruchenko, I. Moore, D. Nesterenko, J. Suhonen, M. Vilén, High-precision electron-capture q value measurement of 111in for electron-neutrino mass determination, Phys. Lett. B 832 (2022) 137226, https://doi.org/10.1016/j.physletb.2022.137226, https://www.sciencedirect.com/science/article/pii/S0370269322003604.

[30] T. Eronen, Z. Ge, A. de Roubin, M. Ramalho, J. Kostensalo, J. Kotila, O. Beliushkina, C. Delafosse, S. Geldhof, W. Gins, M. Hukkanen, A. Jokinen, A. Kankainen, I. Moore, D. Nesterenko, M. Stryjczyk, J. Suhonen, High-precision measurement of a low q value for allowed beta-decay of 131i related to neutrino mass determination, Phys. Lett. B 830 (2022) 137135, https://doi.org/10.1016/j.physletb.2022.137135, https://www.sciencedirect.com/science/article/pii/S0370269322002696.

[31] Z. Ge, T. Eronen, A. de Roubin, J. Kostensalo, J. Suhonen, D.A. Nesterenko, O. Beliuskina, R. de Groote, C. Delafosse, S. Geldhof, W. Gins, M. Hukkanen, A. Jokinen, A. Kankainen, J. Kotila, A. Koszorús, I.D. Moore, A. Raggio, S. Rinta-Antila, V. Virtanen, A.P. Weaver, A. Zadvornaya, Direct determination of the atomic mass difference of the pairs ^{76}As-^{76}Se and ^{155}Tb-^{155}Gd rules out ^{76}As and ^{155}Tb as possible candidates for electron (anti)neutrino mass measurements, Phys. Rev. C 106 (2022) 015502, https://doi.org/10.1103/PhysRevC.106.015502, https://link.aps.org/doi/10.1103/PhysRevC.106.015502.

[32] M. Ramalho, Z. Ge, T. Eronen, D.A. Nesterenko, J. Jaatinen, A. Jokinen, A. Kankainen, J. Kostensalo, J. Kotila, M.I. Krivoruchenko, J. Suhonen, K.S. Tyrin, V. Virtanen, Observation of an ultralow-q-value electron-capture channel decaying to ^{75}As via a high-precision mass measurement, Phys. Rev. C 106 (2022) 015501, https://doi.org/10.1103/PhysRevC.106.015501, https://link.aps.org/doi/10.1103/PhysRevC.106.015501.

[33] N.D. Gamage, R. Sandler, F. Buchinger, J.A. Clark, D. Ray, R. Orford, W.S. Porter, M. Redshaw, G. Savard, K.S. Sharma, A.A. Valverde, Precise q-value measurements of ^{112,113}Ag and ^{115}Cd with the Canadian Penning trap for evaluation of potential ultralow q-value β decays, Phys. Rev. C 106 (2022) 045503, https://doi.org/10.1103/PhysRevC.106.045503, https://link.aps.org/doi/10.1103/PhysRevC.106.045503.

[34] M. Redshaw, Precise q value determinations for forbidden and low energy $$\beta $$-decays using Penning trap mass spectrometry, Eur. Phys. J. A 59 (2) (2023) 18, https://doi.org/10.1140/epja/s10050-023-00925-9.

[35] Z. Ge, T. Eronen, A. de Roubin, M. Ramalho, J. Kostensalo, J. Kotila, J. Suhonen, D.A. Nesterenko, A. Kankainen, P. Ascher, O. Beliuskina, M. Flayol, M. Gerbaux, S. Grévy, M. Hukkanen, A. Husson, A. Jaries, A. Jokinen, I.D. Moore, P. Pirinen, J. Romero, M. Stryjczyk, V. Virtanen, A. Zadvornaya, β^- decay q-value measurement of ^{136}Cs and its implications for neutrino studies, Phys. Rev. C 108 (2023) 045502, https://doi.org/10.1103/PhysRevC.108.045502, https://link.aps.org/doi/10.1103/PhysRevC.108.045502.

[36] A.A. Valverde, F.G. Kondev, B. Liu, D. Ray, M. Brodeur, D.P. Burdette, N. Callahan, A. Cannon, J.A. Clark, D.E.M. Hoff, R. Orford, W.S. Porter, K.S. Sharma, L. Varriano, Precise mass measurements of a = 133 isobars with the Canadian Penning trap: resolving the q anomaly at 133te, https://arxiv.org/abs/2312.06903, 2024, arXiv:2312.06903.

[37] Z. Ge, T. Eronen, M. Ramalho, A. de Roubin, D.A. Nesterenko, A. Kankainen, O. Beliuskina, R. de Groote, S. Geldhof, W. Gins, M. Hukkanen, A. Jokinen, Á. Koszorús, J. Kotila, J. Kostensalo, I.D. Moore, P. Pirinen, A. Raggio, S. Rinta-Antila, V.A. Sevestrean, J. Suhonen, V. Virtanen, A. Zadvornaya, Direct high-precision measurement of the mass difference of 77*As*-77*Se* related to neutrino mass determination, Eur. Phys. J. A 60 (5) (2024) 104, https://doi.org/10.1140/epja/s10050-024-01317-3.

[38] D. Carney, K.G. Leach, D.C. Moore, Searches for massive neutrinos with mechanical quantum sensors, PRX Quantum 4 (2023) 010315, https://doi.org/10.1103/PRXQuantum.4.010315, https://link.aps.org/doi/10.1103/PRXQuantum.4.010315.

[39] T. Eronen, J.C. Hardy, High-precision Q_{EC}-value measurements for superallowed decays, Eur. Phys. J. A 48 (4) (2012) 1–8, https://doi.org/10.1140/epja/i2012-12048-y.

[40] I.D. Moore, T. Eronen, D. Gorelov, J. Hakala, A. Jokinen, A. Kankainen, V.S. Kolhinen, J. Koponen, H. Penttilä, I. Pohjalainen, M. Reponen, J. Rissanen, A. Saastamoinen, S. Rinta-Antila, V. Sonnenschein, J. Äystö, Towards commissioning the new IGISOL-4 facility, Nucl. Instrum. Methods Phys. Res., Sect. B, Beam Interact. Mater. Atoms 317 (PART B) (2013) 208–213, https://doi.org/10.1016/j.nimb.2013.06.036, http://www.sciencedirect.com/science/article/pii/S0168583X13007143.

[41] V.S. Kolhinen, T. Eronen, D. Gorelov, J. Hakala, A. Jokinen, K. Jokiranta, A. Kankainen, M. Koikkalainen, J. Koponen, H. Kulmala, M. Lantz, A. Mattera, I.D. Moore, H. Penttilä, T. Pikkarainen, I. Pohjlainen, M. Reponen, S. Rinta-Antila, J. Rissanen, C. Rodríguez Triguero, K. Rytkönen, A. Saastamoinen, A. Solders, V. Sonnenschein, J. Äystö, Recommissioning of JYFLTRAP at the new IGISOL-4 facility, Nucl. Instrum. Methods Phys. Res., Sect. B, Beam Interact. Mater. Atoms 317 (PART B) (2013) 506–509, https://doi.org/10.1016/j.nimb.2013.07.050, http://www.sciencedirect.com/science/article/pii/S0168583X13008641.

[42] P. Karvonen, I.D. Moore, T. Sonoda, T. Kessler, H. Penttilä, K. Peräjärvi, P. Ronkanen, J. Äystö, A sextupole ion beam guide to improve the efficiency and beam quality at IGISOL, Nucl. Instrum. Methods Phys. Res., Sect. B, Beam Interact. Mater. Atoms 266 (21) (2008) 4794–4807, https://doi.org/10.1016/j.nimb.2008.07.022, http://www.sciencedirect.com/science/article/B6TJN-4T2S8KR-1/2/1d7624cd369335096dcb1fd81a410fea.

[43] A. Nieminen, J. Huikari, A. Jokinen, J. Äystö, P. Campbell, E.C. Cochrane, Beam cooler for low-energy radioactive ions, Nucl. Instrum. Methods Phys. Res., Sect. A, Accel. Spectrom. Detect. Assoc. Equip. 469 (2) (2001) 244–253, https://doi.org/10.1016/S0168-9002(00)00750-6, http://www.sciencedirect.com/science/article/B6TJM-43PGJKX-C/1/93d5587efba5cfe8571b63228952dab8.

[44] G. Savard, S. Becker, G. Bollen, H.J. Kluge, R.B. Moore, T. Otto, L. Schweikhard, H. Stolzenberg, U. Wiess, A new cooling technique for heavy ions in a Penning trap, Phys. Lett. A 158 (5) (1991) 247–252, https://doi.org/10.1016/0375-9601(91)91008-2.

[45] T. Eronen, V.V. Elomaa, U. Hager, J. Hakala, A. Jokinen, A. Kankainen, S. Rahaman, J. Rissanen, C. Weber, J. Äystö, JYFLTRAP: mass spectrometry and isomerically clean beams, Acta Phys. Pol. B 39 (2) (2008) 445–455, https://www.actaphys.uj.edu.pl/R/39/2/445/pdf.

[46] D.A. Nesterenko, T. Eronen, Z. Ge, A. Kankainen, M. Vilen, Study of radial motion phase advance during motion excitations in a Penning trap and accuracy of jyfltrap mass spectrometer, Eur. Phys. J. A 57 (2021) 302, https://doi.org/10.1140/epja/s10050-021-00608-3.

[47] D.A. Nesterenko, T. Eronen, A. Kankainen, L. Canete, A. Jokinen, I.D. Moore, H. Penttilä, S. Rinta-Antila, A. de Roubin, M. Vilen, Phase-imaging ion-cyclotron-resonance technique at the JYFLTRAP double Penning trap mass spectrometer, Eur. Phys. J. A 54 (9) (2018) 154, https://doi.org/10.1140/epja/i2018-12589-y.

[48] S. Eliseev, K. Blaum, M. Block, A. Dörr, C. Droese, T. Eronen, M. Goncharov, M. Höcker, J. Ketter, E.M. Ramirez, D.A. Nesterenko, Y.N. Novikov, L. Schweikhard, A phase-imaging technique for cyclotron-frequency measurements, Appl. Phys. B, Lasers Opt. 114 (1–2) (2014) 107–128, https://doi.org/10.1007/s00340-013-5621-0.

[49] S. Eliseev, K. Blaum, M. Block, C. Droese, M. Goncharov, E. Minaya Ramirez, D.A. Nesterenko, Y.N. Novikov, L. Schweikhard, Phase-imaging ion-cyclotron-resonance measurements for short-lived nuclides, Phys. Rev. Lett. 110 (8) (2013) 82501, https://doi.org/10.1103/PhysRevLett.110.082501.

[50] A. Kramida, Yu. Ralchenko, J. Reader, NIST ASD Team, NIST Atomic Spectra Database (ver. 5.8), [Online]. Available: https://physics.nist.gov/asd, 2021, January 19, National Institute of Standards and Technology, Gaithersburg, MD, 2020.

[51] M. Wang, W. Huang, F. Kondev, G. Audi, S. Naimi, The AME 2020 atomic mass evaluation (II). tables, graphs and references*, Chin. Phys. C 45 (3) (2021) 030003, https://doi.org/10.1088/1674-1137/abddaf.

[52] National nuclear data center. Available at https://www.nndc.bnl.gov/, 2020/4/7; https://www.nndc.bnl.gov/, 2021.

[53] M. Wiedeking, M. Krtička, L.A. Bernstein, J.M. Allmond, M.S. Basunia, D.L. Bleuel, J.T. Harke, B.H. Daub, P. Fallon, R.B. Firestone, B.L. Goldblum, R. Hatarik, P.T. Lake, A.C. Larsen, I.Y. Lee, S.R. Lesher, S. Paschalis, M. Petri, L. Phair, N.D. Scielzo, A. Volya, γ-ray decay from neutron-bound and unbound states in ^{95}Mo and a novel technique for spin determination, Phys. Rev. C 93 (2016) 024303, https://doi.org/10.1103/PhysRevC.93.024303, https://link.aps.org/doi/10.1103/PhysRevC.93.024303.

[54] S.K. Basu, G. Mukherjee, A.A. Sonzogni, Nuclear data sheets for A = 95, Nucl. Data Sheets 111 (10–11) (2010) 2555–2737, https://doi.org/10.1016/j.nds.2010.10.001.

[55] A. Thompson, I. Lindau, D. Attwood, Y. Liu, E. Gullikson, P. Pianetta, M. Howells, A. Robinson, K. Kim, J. Scofield, J. Kirz, J. Underwood, J. Kortright, G. Wiliams, H. Winick, X-ray Data Booklet, Lawrence Berkeley National Laboratory, Berkeley, California, 2009.

[56] A. Kellerbauer, K. Blaum, G. Bollen, F. Herfurth, H.J. Kluge, M. Kuckein, E. Sauvan, C. Scheidenberger, L. Schweikhard, From direct to absolute mass measurements: a study of the accuracy of ISOLTRAP, Eur. Phys. J. D 22 (1) (2003) 53–64, https://doi.org/10.1140/epjd/e2002-00222-0.

[57] C. Roux, K. Blaum, M. Block, C. Droese, S. Eliseev, M. Goncharov, F. Herfurth, E.M. Ramirez, D.A. Nesterenko, Y.N. Novikov, L. Schweikhard, Data analysis of Q-value measurements for double-electron capture with SHIPTRAP, Eur. Phys. J. D 67 (7) (2013) 1–9, https://doi.org/10.1140/epjd/e2013-40110-x.

[58] R.T. Birge, The calculation of errors by the method of least squares, Phys. Rev. 40 (2) (1932) 207–227, https://doi.org/10.1103/PhysRev.40.207, http://link.aps.org/abstract/PR/v40/p207.

[59] W. Huang, M. Wang, F. Kondev, G. Audi, S. Naimi, The AME 2020 atomic mass evaluation (I). evaluation of input data, and adjustment procedures*, Chin. Phys. C 45 (3) (2021) 030002, https://doi.org/10.1088/1674-1137/abddb0.

[60] L.M. Langer, D.E. Wortman, Radioactive decay of nb^{95}, Phys. Rev. 132 (1963) 324–328, https://doi.org/10.1103/PhysRev.132.324, https://link.aps.org/doi/10.1103/PhysRev.132.324.

[61] T. Cretzu, K. Hohmuth, J. Schintlmeister, Der zerfall von tc95m, Nucl. Phys. 70 (1) (1965) 129–140, https://doi.org/10.1016/0029-5582(65)90229-4, https://www.sciencedirect.com/science/article/pii/0029558265902294.

[62] N.M. Antoneva, A.V. Barkov, A.V. Zolotavin, P.P. Dmitriev, S.V. Kamynov, G.S. Katykhin, E.T. Kondrat, N.I. Krasnov, Y.N. Podkopaev, V.A. Sergienko, V.I. Fominykh, The decay of ^{95}*tc, Izv. Akad. Nauk SSSR, Ser. Fiz. 38 (1974) 48.

[63] J.A. Pinston, E. Monnand, A. Moussa, Desintegration de ^{95}ru, J. Phys. (Paris) 29 (1968) 257.

[64] B. Brown, W. Rae, The shell-model code NuShellX@MSU, Nucl. Data Sheets 120 (2014) 115–118, https://doi.org/10.1016/j.nds.2014.07.022.

[65] V.A. Sevestrean, O. Nițescu, S. Ghinescu, S. Stoica, Self-consistent calculations for atomic electron capture, Phys. Rev. A 108 (2023) 012810, https://doi.org/10.1103/PhysRevA.108.012810, https://link.aps.org/doi/10.1103/PhysRevA.108.012810.

[66] F. Salvat, J.M. Fernández-Varea, Radial: a fortran subroutine package for the solution of the radial Schrödinger and Dirac wave equations, Comput. Phys. Commun. 240 (2019) 165–177, https://doi.org/10.1016/j.cpc.2019.02.011, https://www.sciencedirect.com/science/article/pii/S0010465519300633.

[67] J. Campbell, T. Papp, Widths of the atomic k–n7 levels, At. Data Nucl. Data Tables 77 (1) (2001) 1–56, https://doi.org/10.1006/adnd.2000.0848, https://www.sciencedirect.com/science/article/pii/S0092640X00908489.

[68] H. Behrens, W. Bühring, Electron Radial Wave Functions and Nuclear Beta-Decay, International Series of Monographs on Physics, Clarendon Press, Oxford, 1982.

[69] J. Suhonen, From Nucleons to Nucleus, Springer, Gaithersburg MD, 20899, Springer–Verlag Berlin Heidelberg, 2007, https://www.springer.com/gp/book/9783540488590#aboutBook.

[70] R. Machleidt, High-precision, charge-dependent bonn nucleon-nucleon potential, Phys. Rev. C 63 (2) (2001) 024001, https://doi.org/10.1103/physrevc.63.024001.

[71] V. Vaquero, A. Jungclaus, T. Aumann, J. Tscheuschner, E.V. Litvinova, J.A. Tostevin, H. Baba, D.S. Ahn, R. Avigo, K. Boretzky, A. Bracco, C. Caesar, F. Camera, S. Chen, V. Derya, P. Doornenbal, J. Endres, N. Fukuda, U. Garg, A. Giaz, M.N. Harakeh, M. Heil, A. Horvat, K. Ieki, N. Imai, N. Inabe, N. Kalantar-Nayestanaki, N. Kobayashi, Y. Kondo, S. Koyama, T. Kubo, I. Martel, M. Matsushita, B. Million, T. Motobayashi, T. Nakamura, N. Nakatsuka, M. Nishimura, S. Nishimura, S. Ota, H. Otsu, T. Ozaki, M. Petri, R. Reifarth, J.L. Rodríguez-Sánchez, D. Rossi, A.T. Saito, H. Sakurai, D. Savran, H. Scheit, F. Schindler, P. Schrock, D. Semmler, Y. Shiga, M. Shikata, Y. Shimizu, H. Simon, D. Steppenbeck, H. Suzuki, T. Sumikama, D. Symochko, I. Syndikus, H. Takeda, S. Takeuchi, R. Taniuchi, Y. Togano, J. Tsubota, H. Wang, O. Wieland, K. Yoneda, J. Zenihiro, A. Zilges, Fragmentation of single-particle strength around the doubly magic nucleus ^{132}Sn and the position of the $0f_{5/2}$ proton-hole state in ^{131}In, Phys. Rev. Lett. 124 (2020) 022501, https://doi.org/10.1103/PhysRevLett.124.022501, https://link.aps.org/doi/10.1103/PhysRevLett.124.022501.

[72] A.F. Lisetskiy, B.A. Brown, M. Horoi, H. Grawe, New $t = 1$ effective interactions for the $f_{5/2}$ $p_{3/2}$ $p_{1/2}$ $g_{9/2}$ model space: implications for valence-mirror symmetry and seniority isomers, Phys. Rev. C 70 (2004) 044314, https://doi.org/10.1103/PhysRevC.70.044314, https://link.aps.org/doi/10.1103/PhysRevC.70.044314.

[73] H. Mach, E.K. Warburton, R.L. Gill, R.F. Casten, J.A. Becker, B.A. Brown, J.A. Winger, Meson-exchange enhancement of the first-forbidden ^{96}Y$^{g}(0^{-})\rightarrow{}^{96}$Zr^{g} (0^{+}) β transition: β decay of the low-spin isomer of ^{96}Y, Phys. Rev. C 41 (1990) 226–242, https://doi.org/10.1103/PhysRevC.41.226, https://link.aps.org/doi/10.1103/PhysRevC.41.226.

[74] M. Honma, T. Otsuka, T. Mizusaki, M. Hjorth-Jensen, Effective interaction for f5pg9-shell nuclei and two-neutrino double beta-decay matrix elements, J. Phys. Conf. Ser. 49 (1) (2006) 45, https://doi.org/10.1088/1742-6596/49/1/011.

[75] J. Barea, J. Kotila, F. Iachello, Nuclear matrix elements for double-β decay, Phys. Rev. C 87 (2013) 014315, https://doi.org/10.1103/PhysRevC.87.014315, https://link.aps.org/doi/10.1103/PhysRevC.87.014315.

[76] J.T. Suhonen, Value of the axial-vector coupling strength in β and $\beta\beta$ decays: a review, Front. Phys. 5 (2017), https://doi.org/10.3389/fphy.2017.00055, https://www.frontiersin.org/articles/10.3389/fphy.2017.00055.

[77] V.A. Sevestrean, M. Ramalho, J. Suhonen, T. Eronen, Z. Ge, O. Niţescu, S. Ghinescu, S. Stoica, A. Kankainen, J. Kotila, J. Kostensalo, et al., 2024, submitted for publication.

[78] C. Schweiger, M. Braß, V. Debierre, M. Door, H. Dorrer, C.E. Düllmann, C. Enss, P. Filianin, L. Gastaldo, Z. Harman, M.W. Haverkort, J. Herkenhoff, P. Indelicato, C.H. Keitel, K. Kromer, D. Lange, Y.N. Novikov, D. Renisch, A. Rischka, R.X. Schüssler, S. Eliseev, K. Blaum, Penning-trap measurement of the q value of electron capture in 163ho for the determination of the electron neutrino mass, Nat. Phys. (2024), https://doi.org/10.1038/s41567-024-02461-9.